Solid Earth

Supplement of

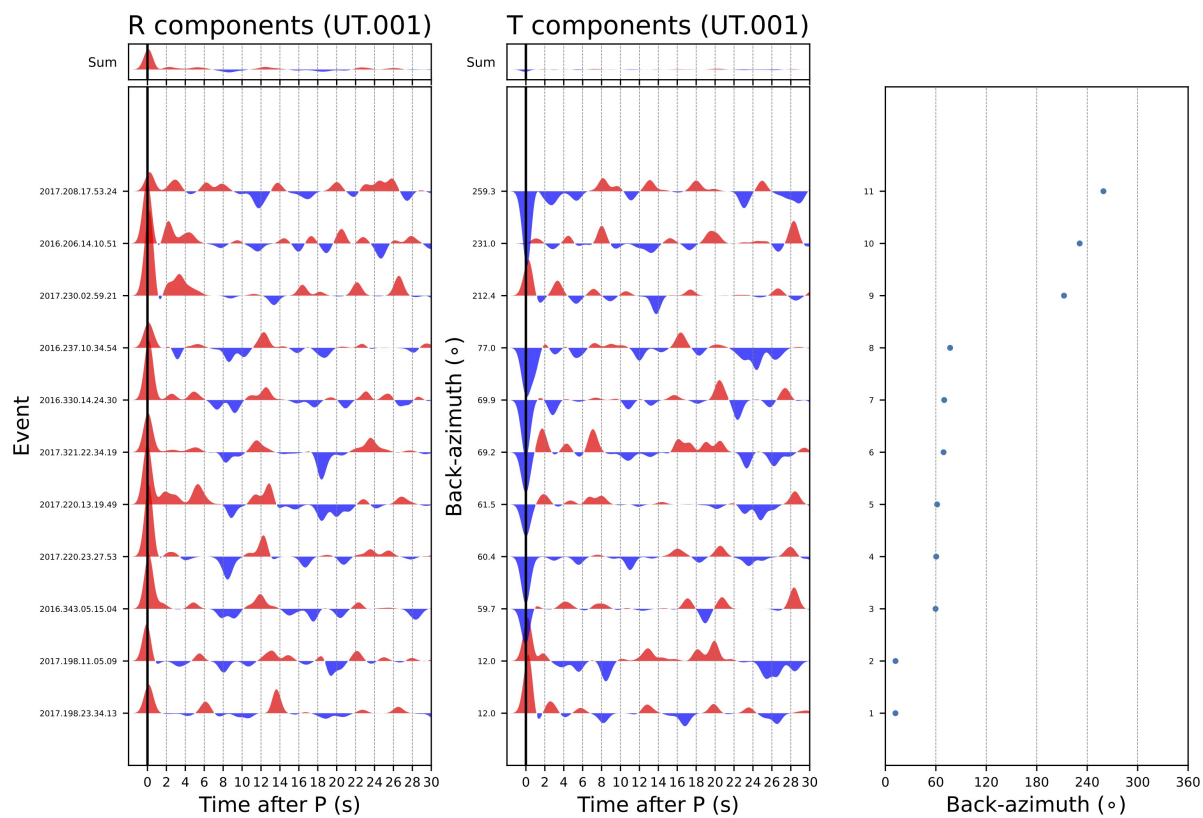# On the crustal composition of the Sardinia–Corsica continental block inferred from receiver functions

Fabio Cammarano et al.

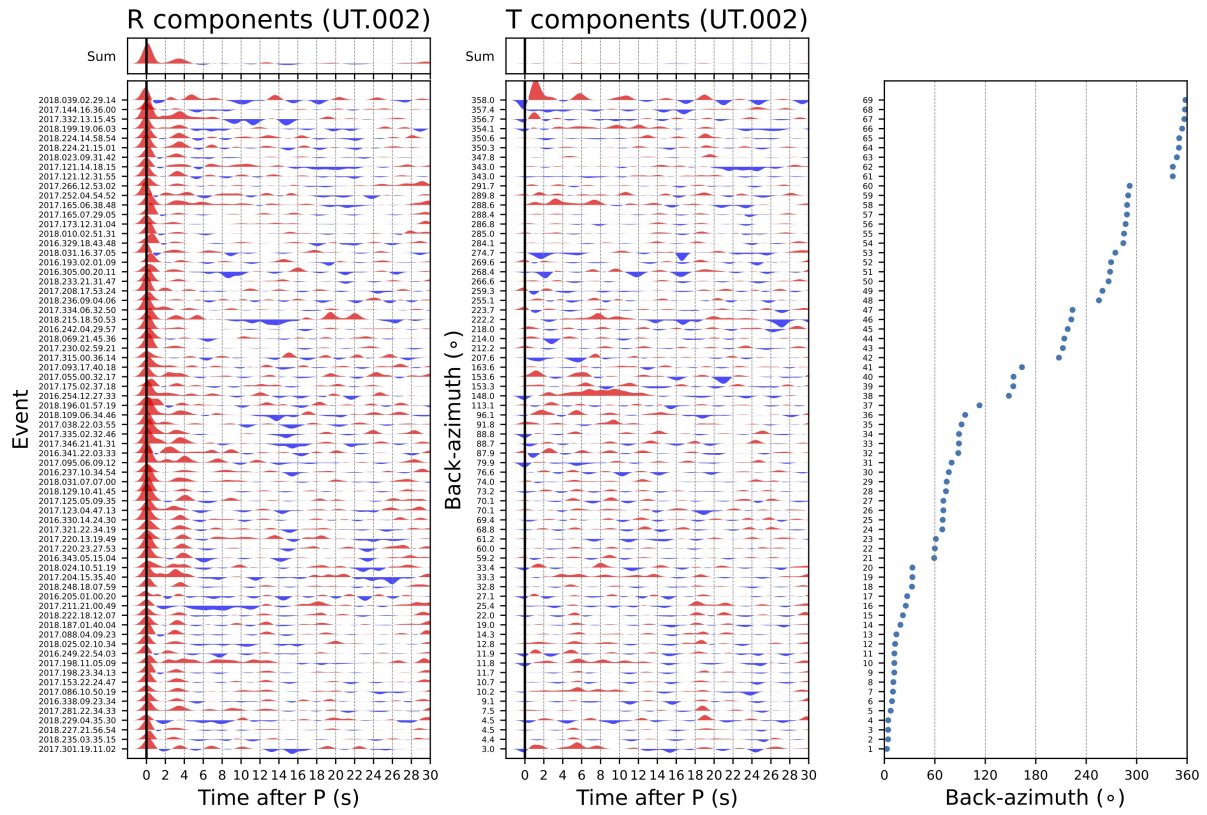*Correspondence to:* Fabio Cammarano (fabio.cammarano@uniroma3.it)

Supporting figures

Figure S1. Radial and transverse P-wave receiver functions for LiSard station UT.001 (LA Maddalena). Panels at the right show the backazimuth of the recorded events.
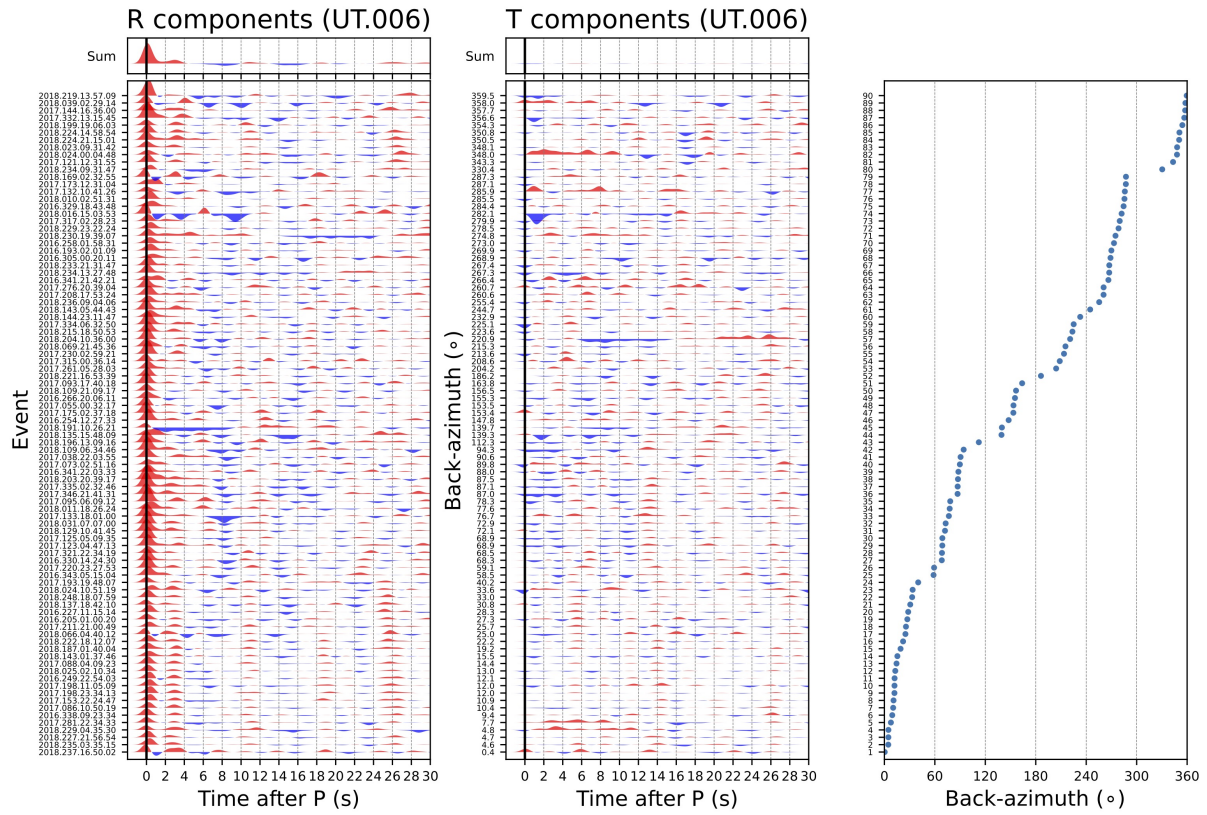
Figure S2. Radial and transverse P-wave receiver functions for LiSard station UT.002 (Oschiri). Panels at the right show the backazimuth of the recorded events.
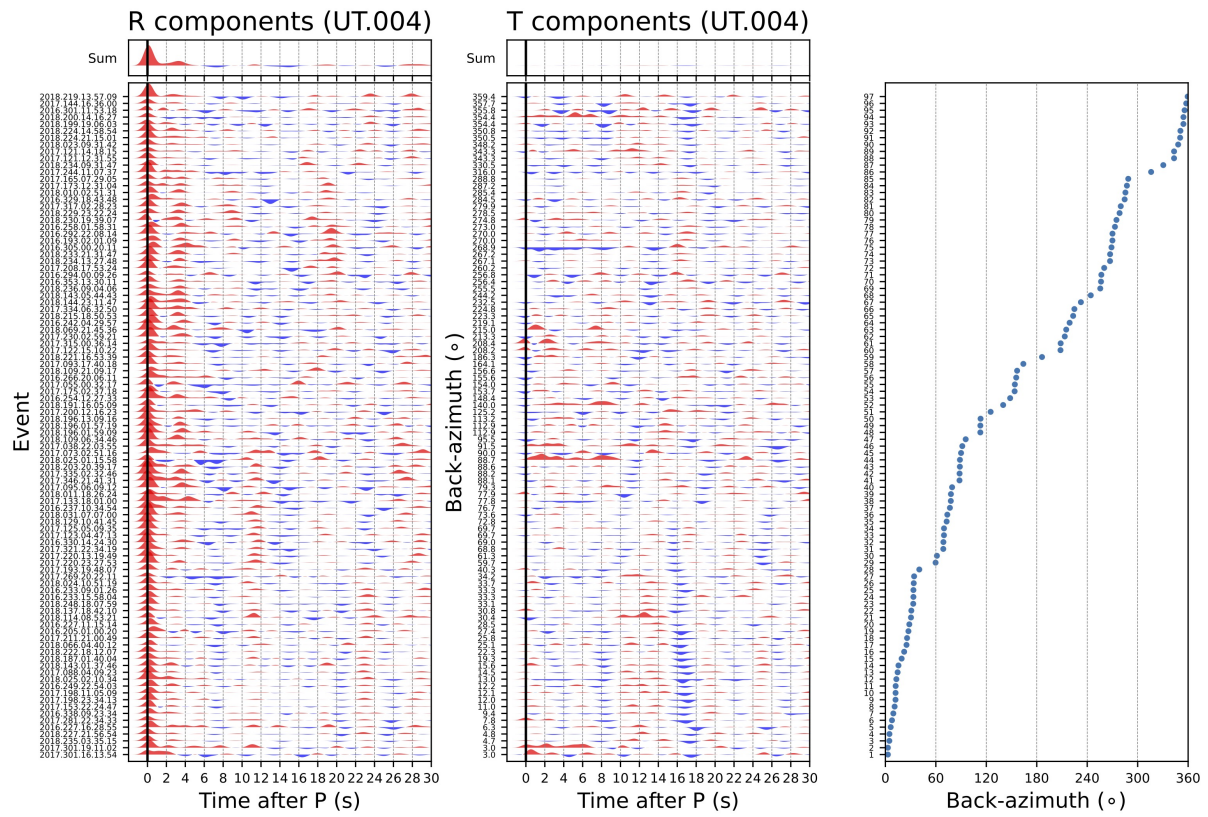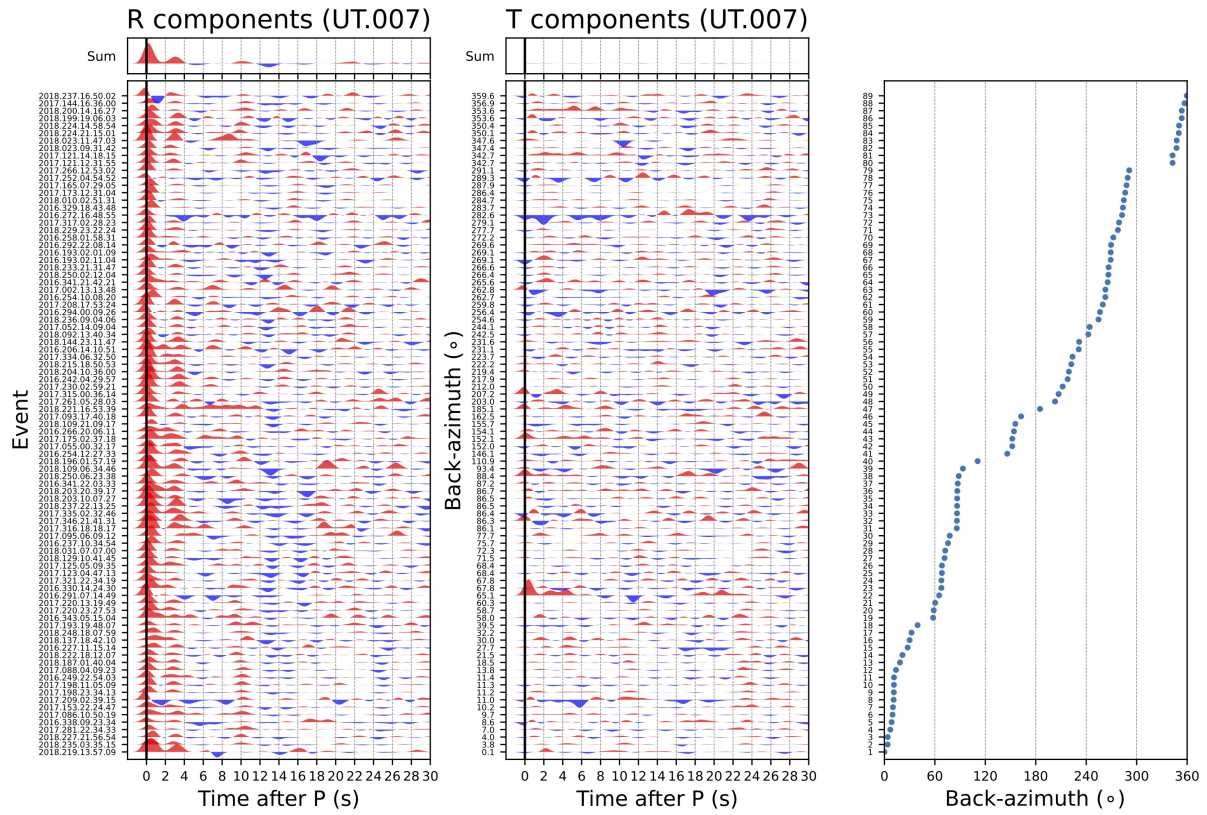
Figure S3. Radial and transverse P-wave receiver functions for LiSard station UT.004 (Lotzorai). Panels at the right show the backazimuth of the recorded events.
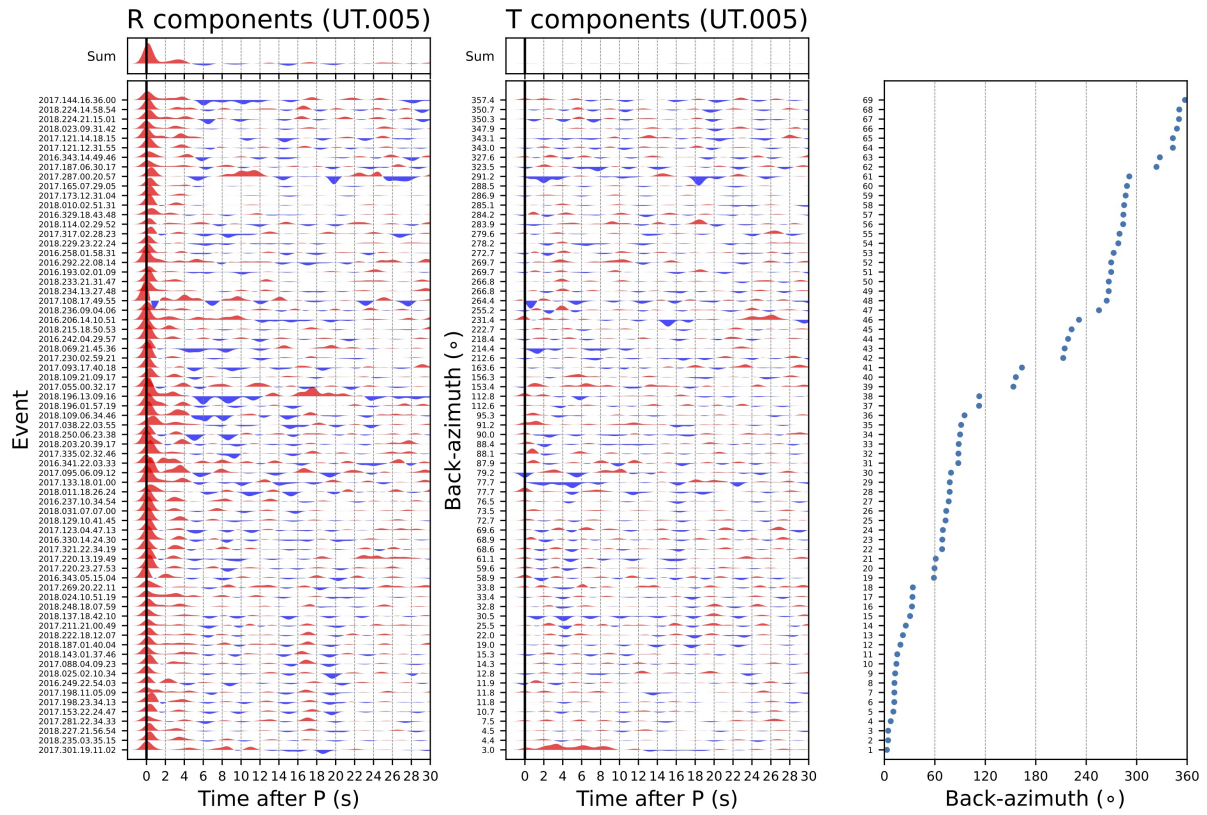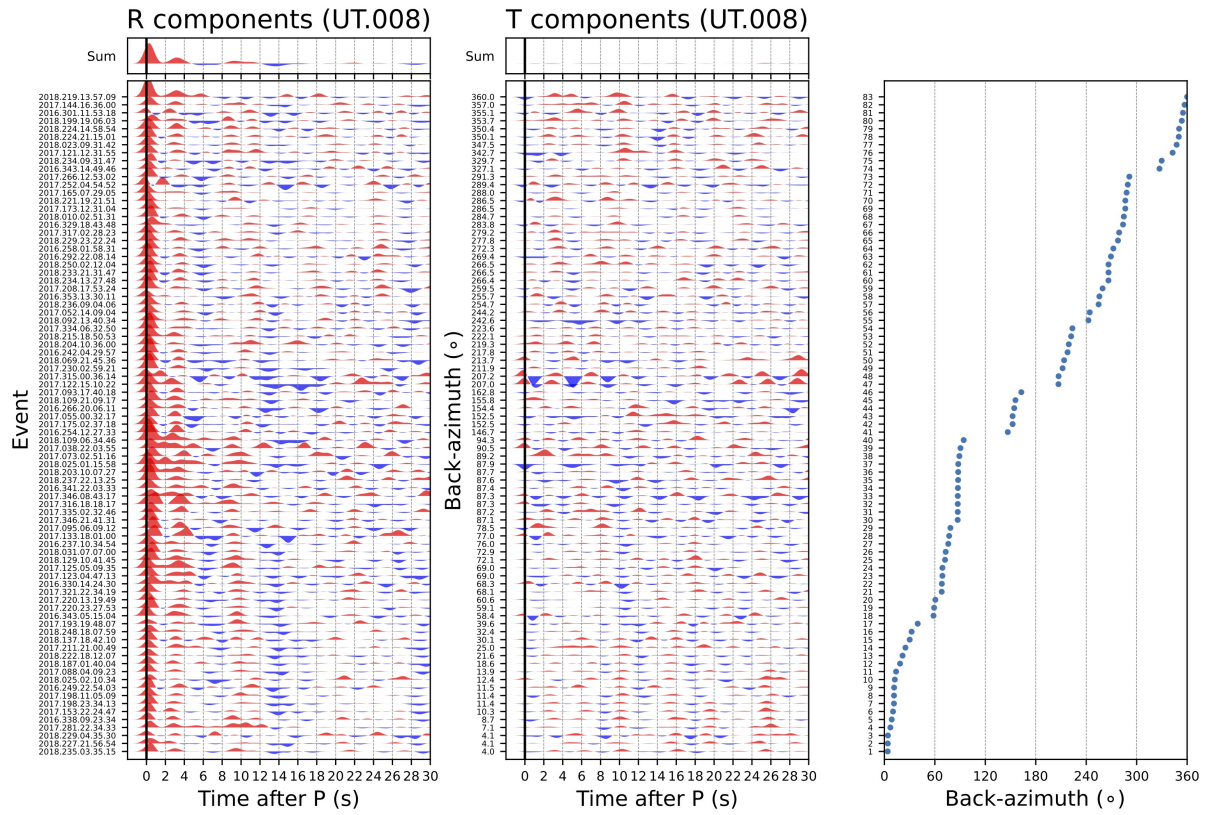
Figure S4. Radial and transverse P-wave receiver functions for LiSard station UT.005 (Ovodda). Panels at the right show the backazimuth of the recorded events.

Figure S5. Radial and transverse P-wave receiver functions for LiSard station UT.006 (Villasimius). Panels at the right show the backazimuth of the recorded events.
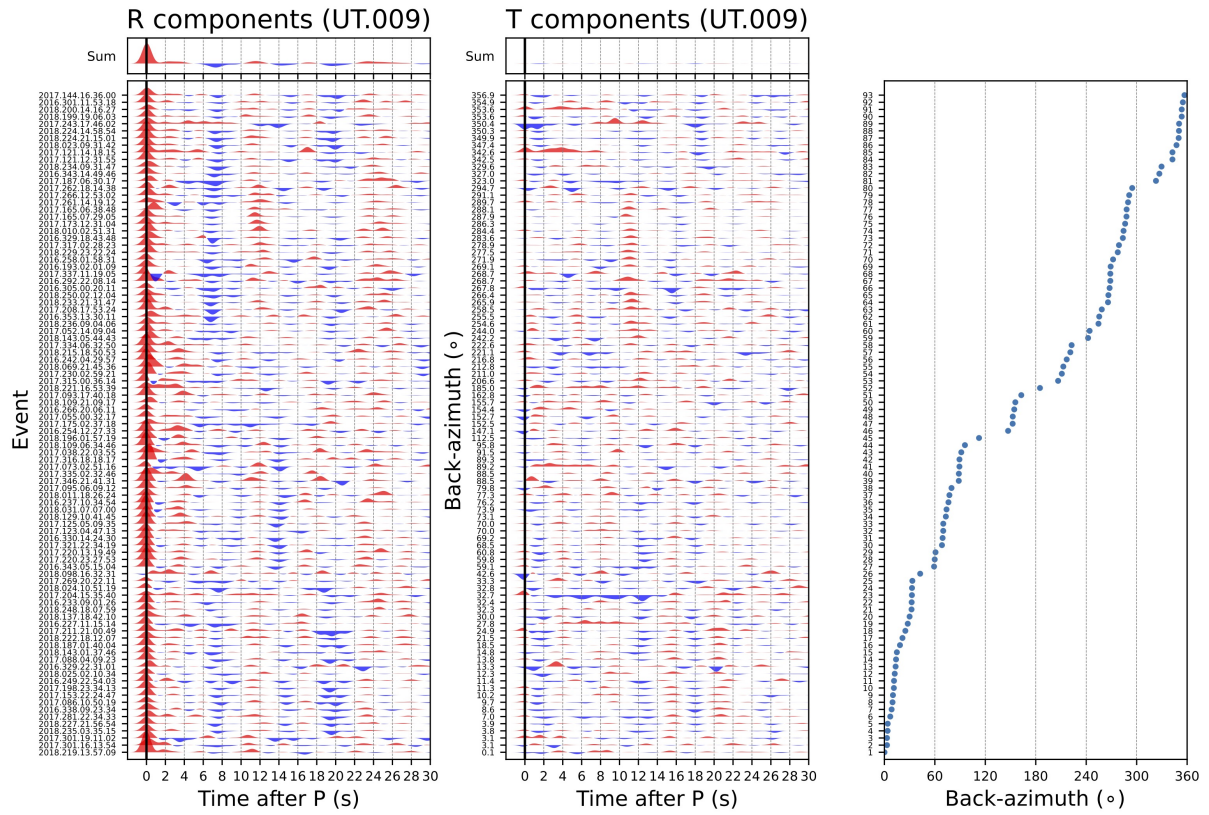
Figure S6. Radial and transverse P-wave receiver functions for LiSard station UT.007 (Carloforte). Panels at the right show the backazimuth of the recorded events.
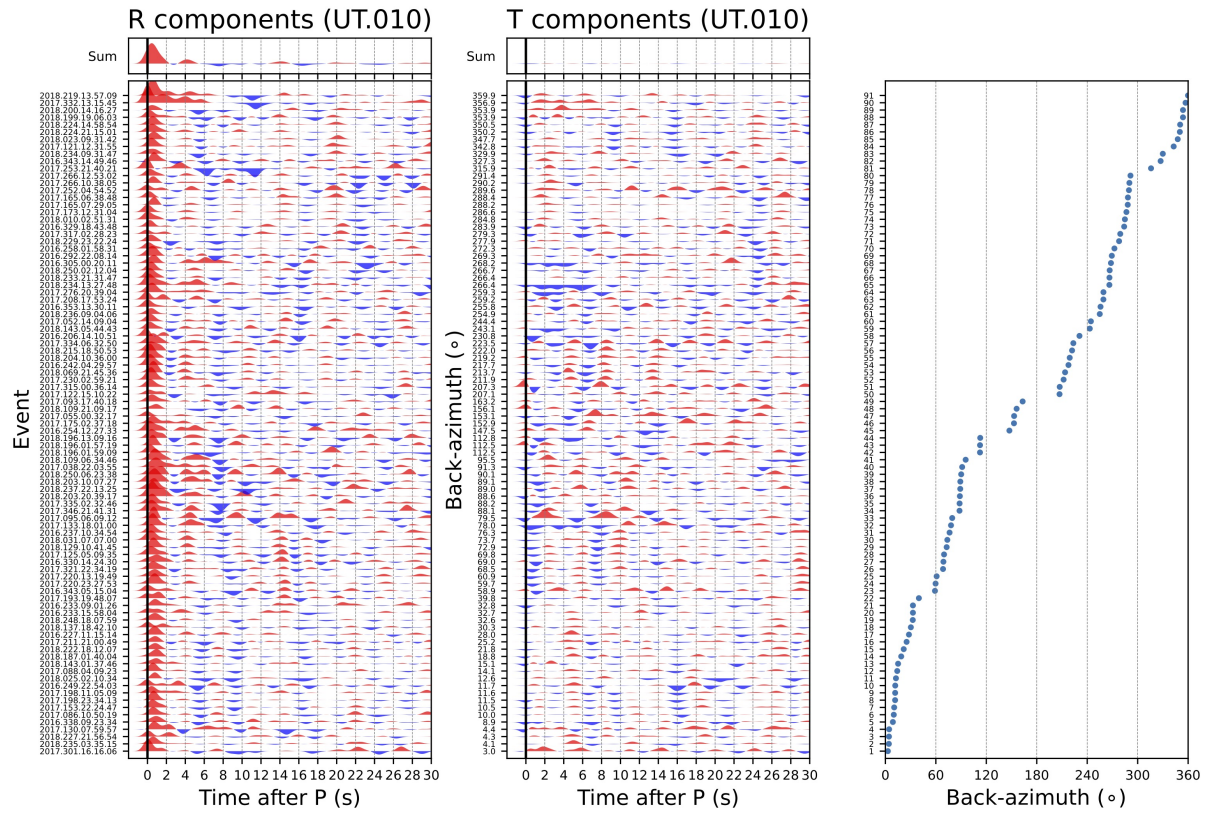
7

Figure S7. Radial and transverse P-wave receiver functions for LiSard station UT.008 (Capofrasca). Panels at the right show the backazimuth of the recorded events.
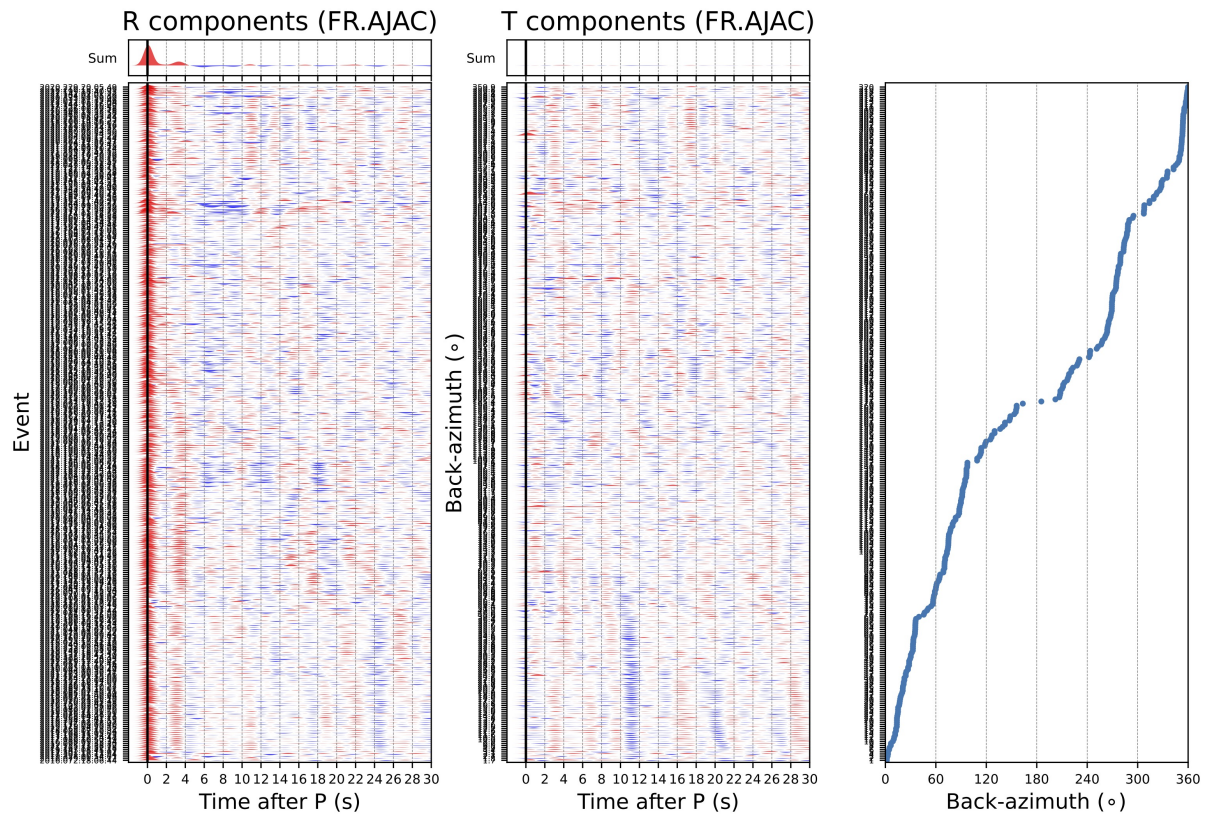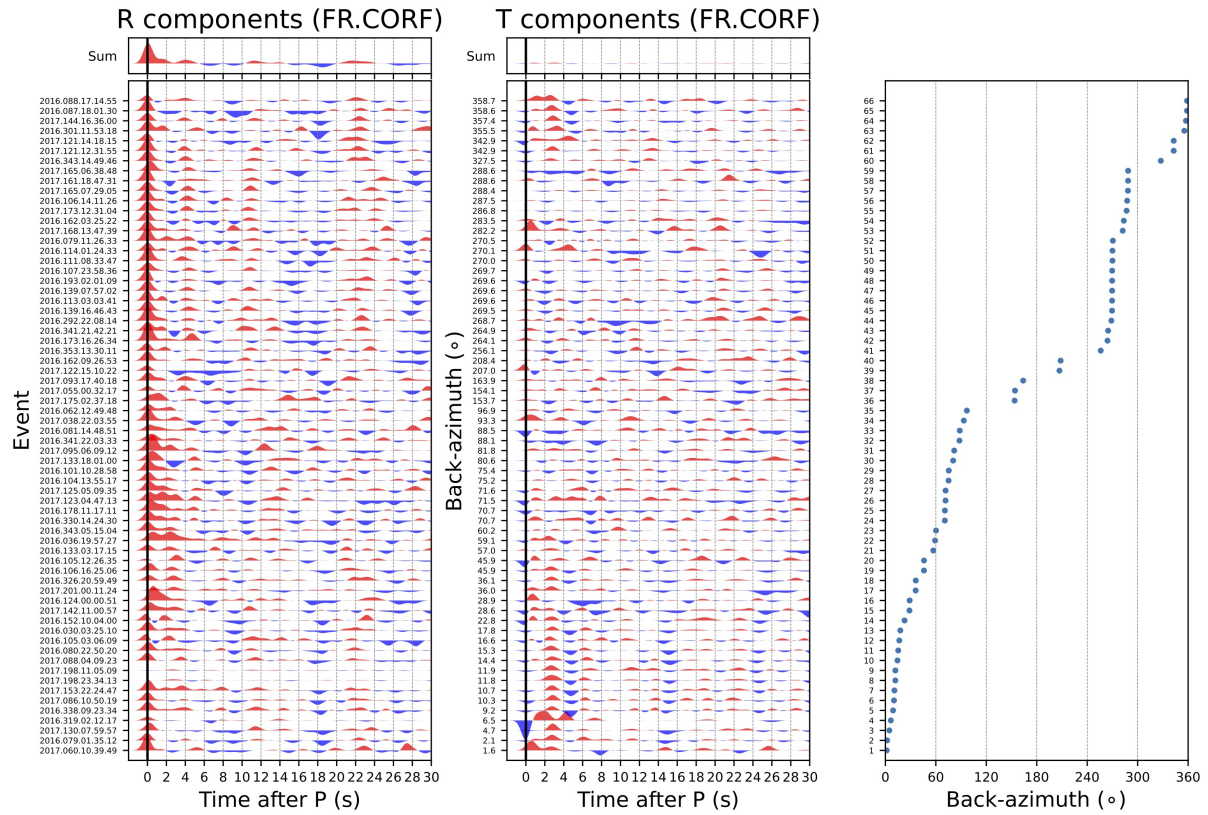
Figure S8. Radial and transverse P-wave receiver functions for LiSard station UT.009 (Asinara). Panels at the right show the backazimuth of the recorded events.
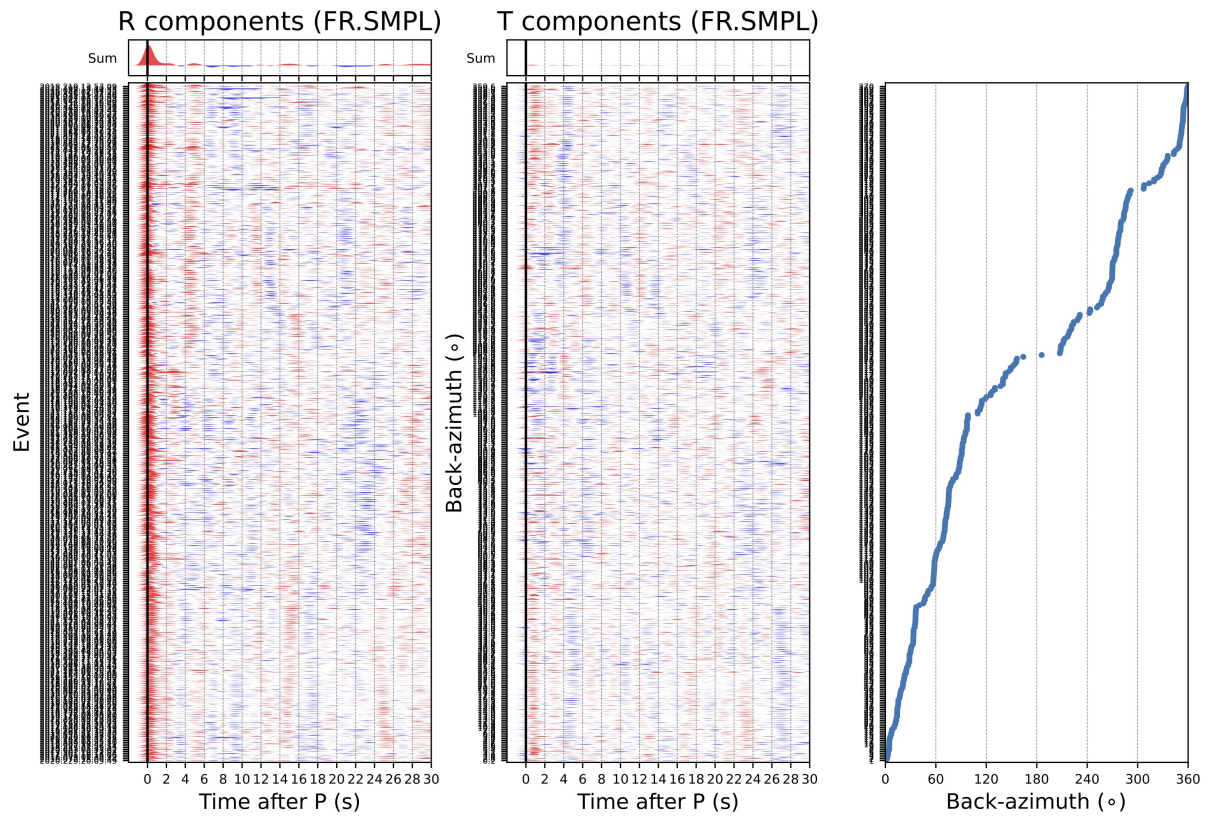
Figure S9. Radial and transverse P-wave receiver functions for LiSard station UT.010 (Giave). Panels at the right show the backazimuth of the recorded events.
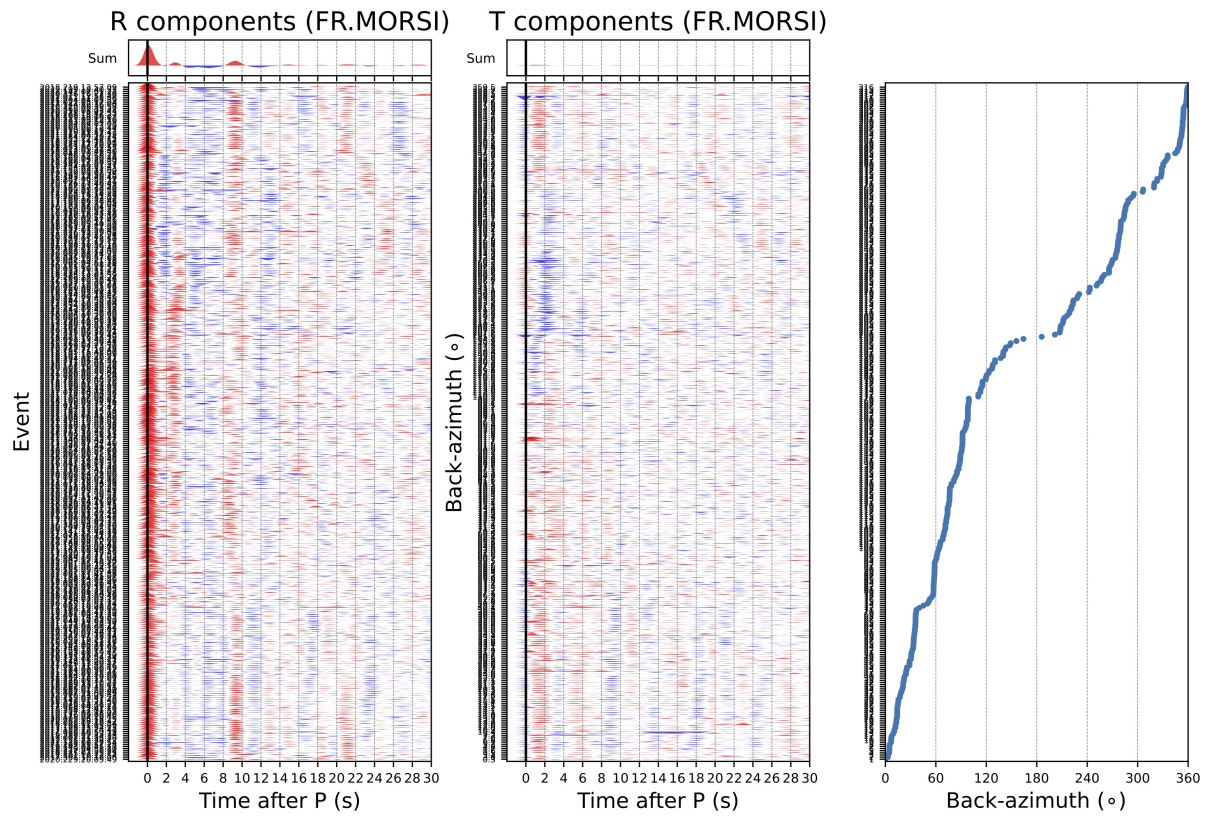
10

Figure S10. Radial and transverse P-wave receiver functions for FR station AJAC (Ajaccio). Panels at the right show the backazimuth of the recorded events.
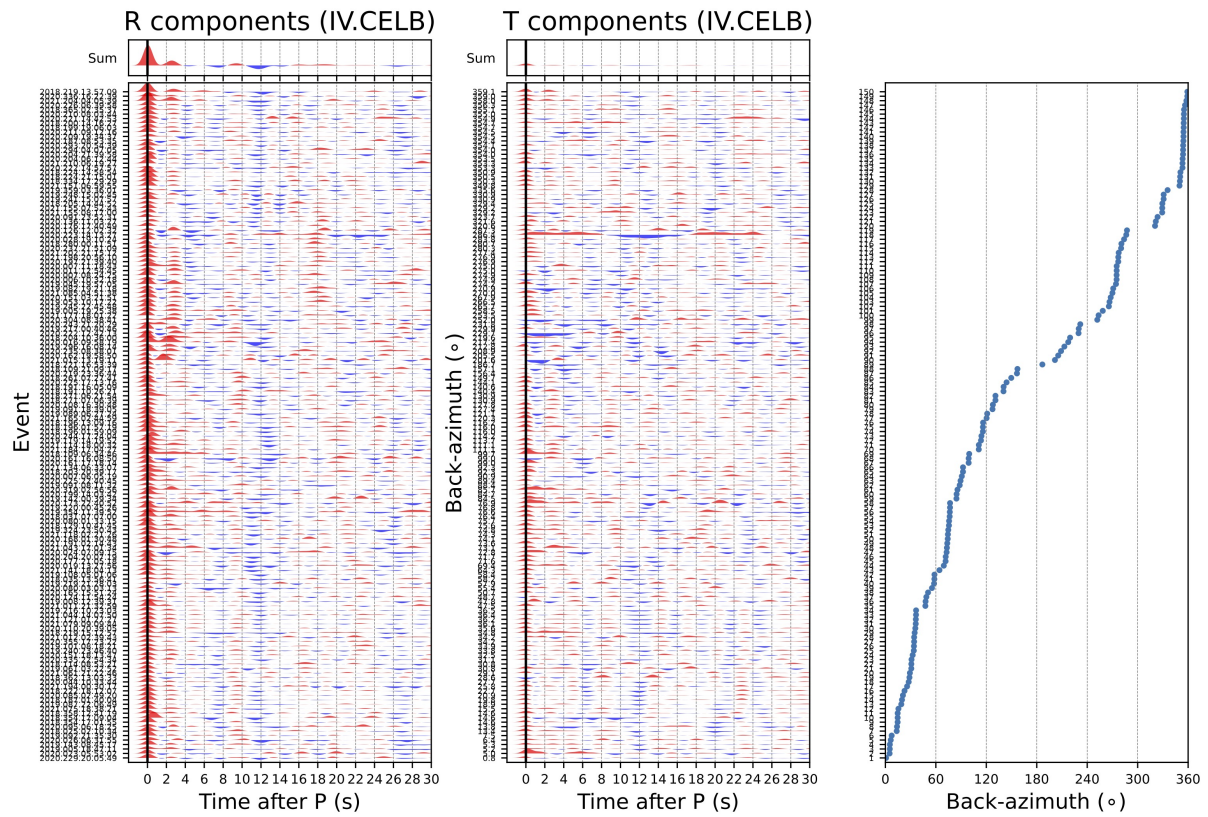
Figure S11. Radial and transverse P-wave receiver functions for FR station CORF (Corte). Panels at the right show the backazimuth of the recorded events.
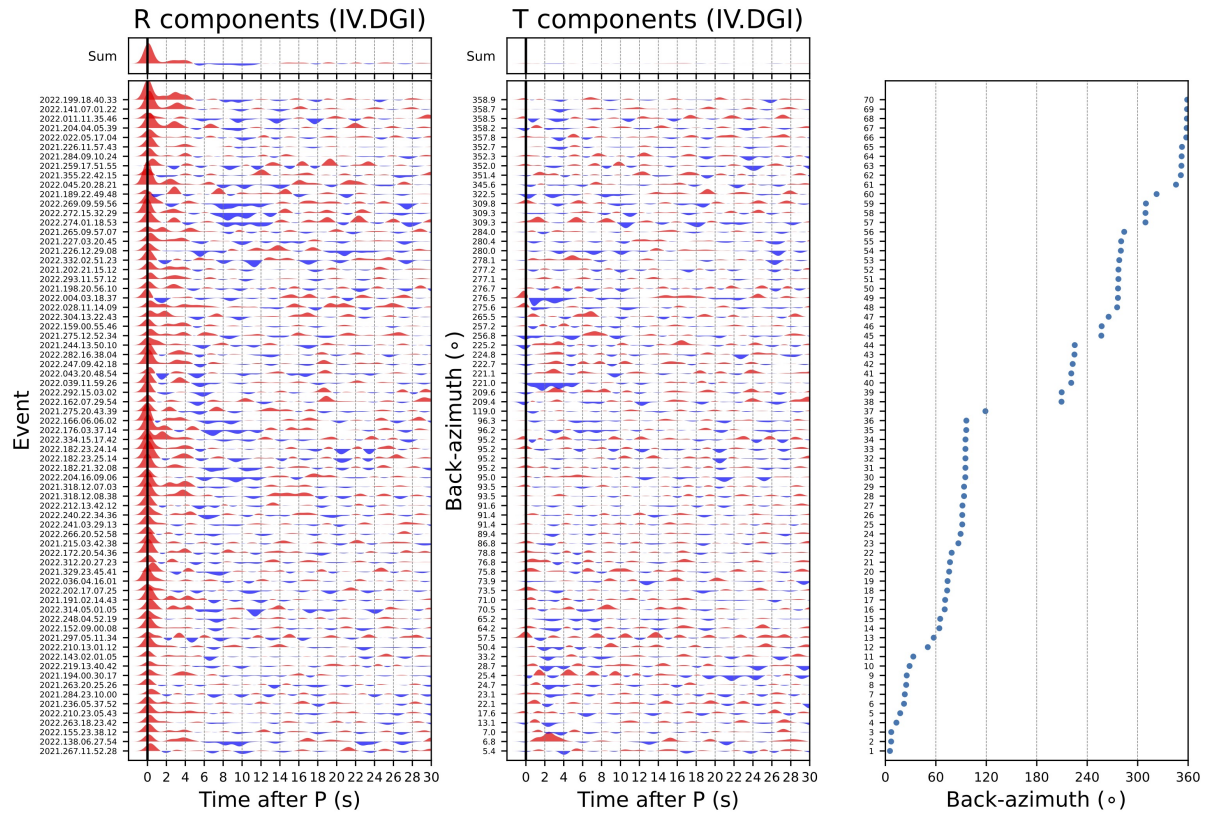
Figure S12. Radial and transverse P-wave receiver functions for FR station SMPL (barrage de Sampolo). Panels at the right show the backazimuth of the recorded events.

Figure S13. Radial and transverse P-wave receiver functions for FR station MORSI (Morsiglia). Panels at the right show the backazimuth of the recorded events.
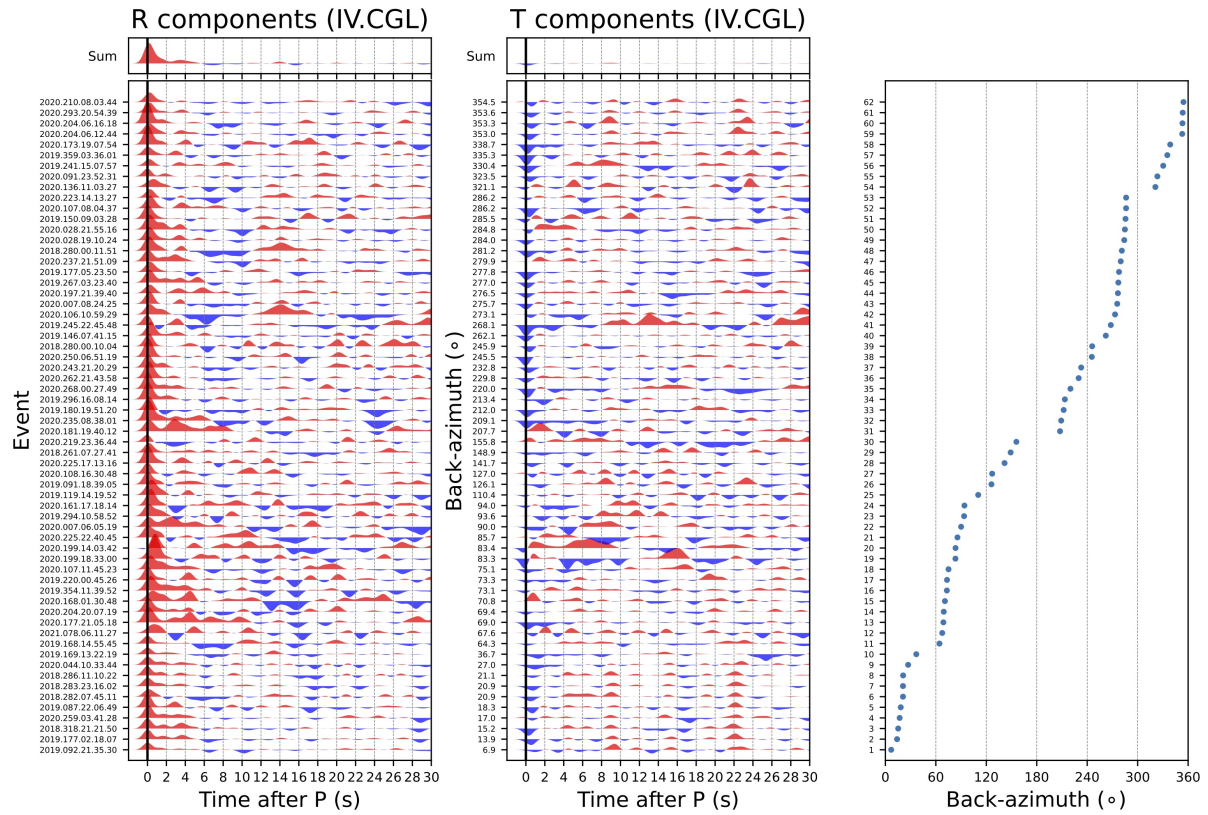
Figure S14. Radial and transverse P-wave receiver functions for IV station CELB (isole d'Elba). Panels at the right show the backazimuth of the recorded events.
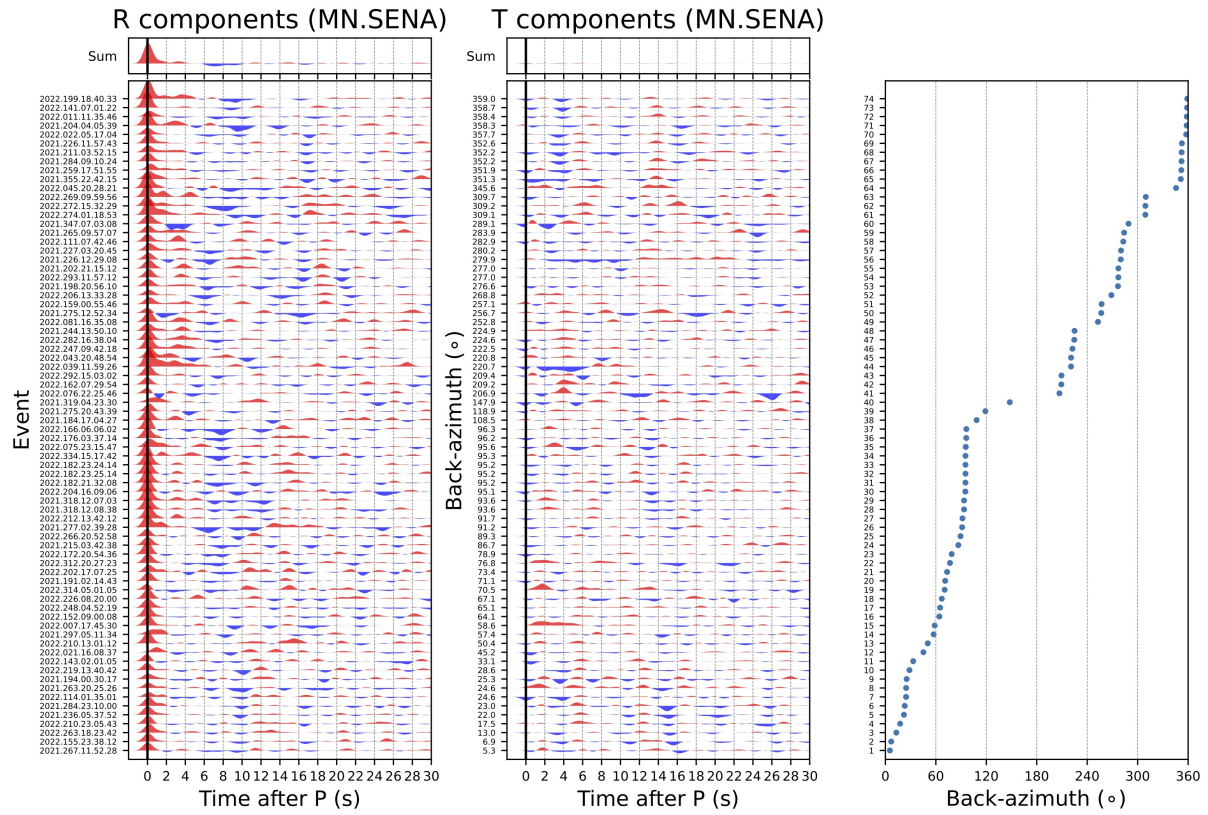
Figure S15. Radial and transverse P-wave receiver functions for IV station DGI (Dorgali). Panels at the right show the backazimuth of the recorded events.
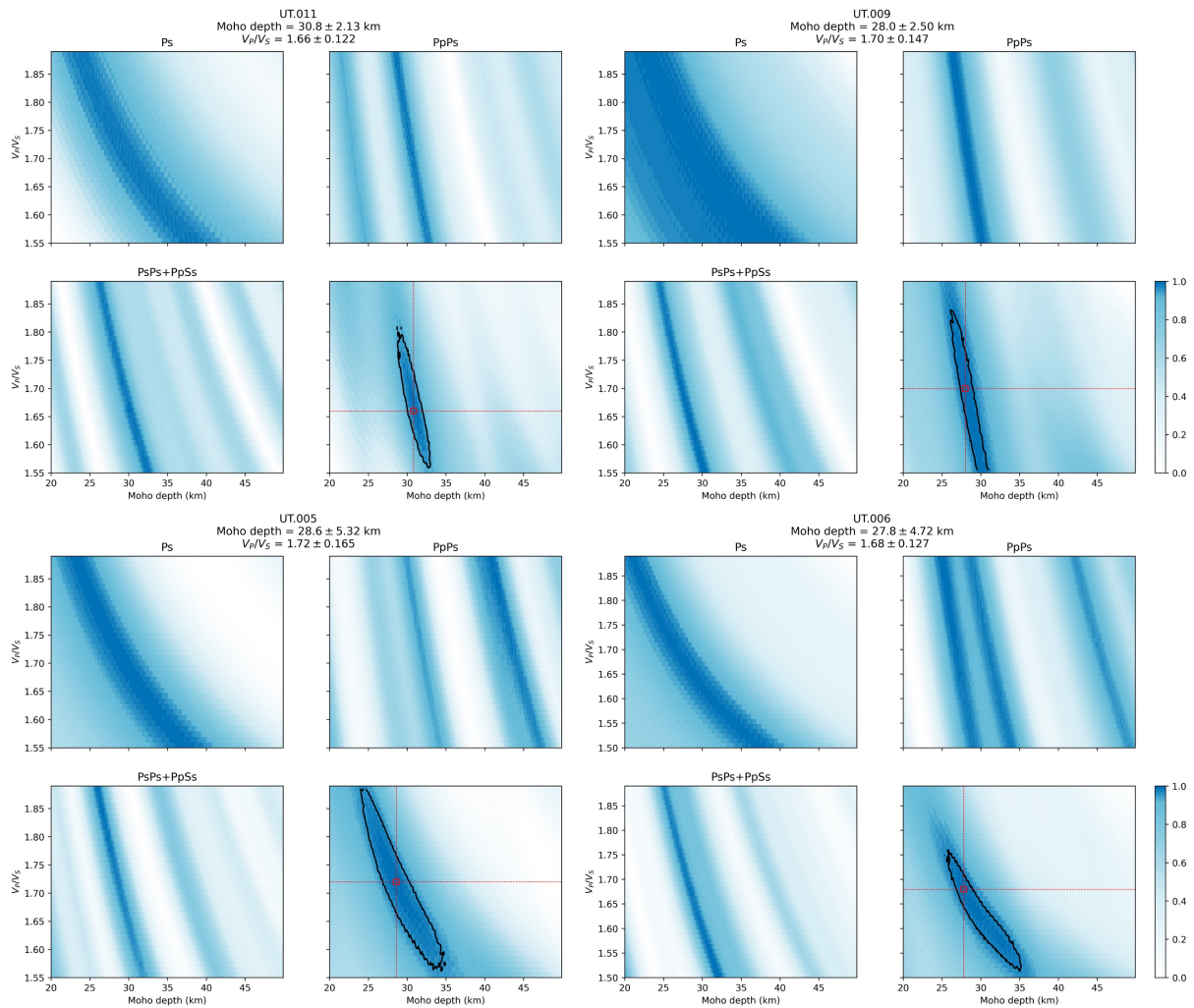
Figure S16. Radial and transverse P-wave receiver functions for IV station CGL (Punta Serpeddi). Panels at the right show the backazimuth of the recorded events.

Figure S17. Radial and transverse P-wave receiver functions for MN station SENA (Sos Enattos). Panels at the right show the backazimuth of the recorded events.
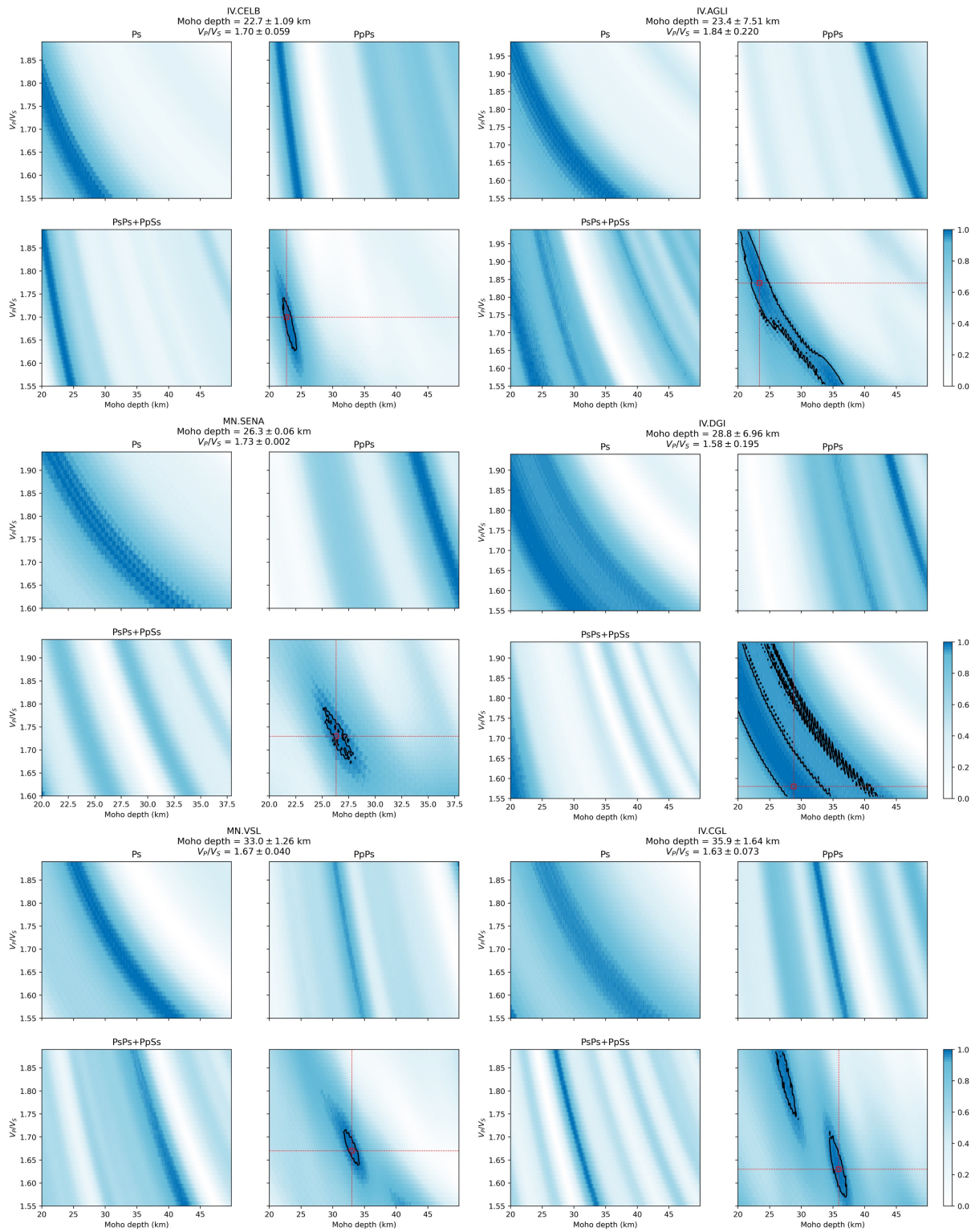
Figure S18. Results of the H-k stacking process for 011, 009, 005 and 006 Lisard stations, all showing intricate features (see main text for details). Stack values in each panel are normalized from 0 to 1.
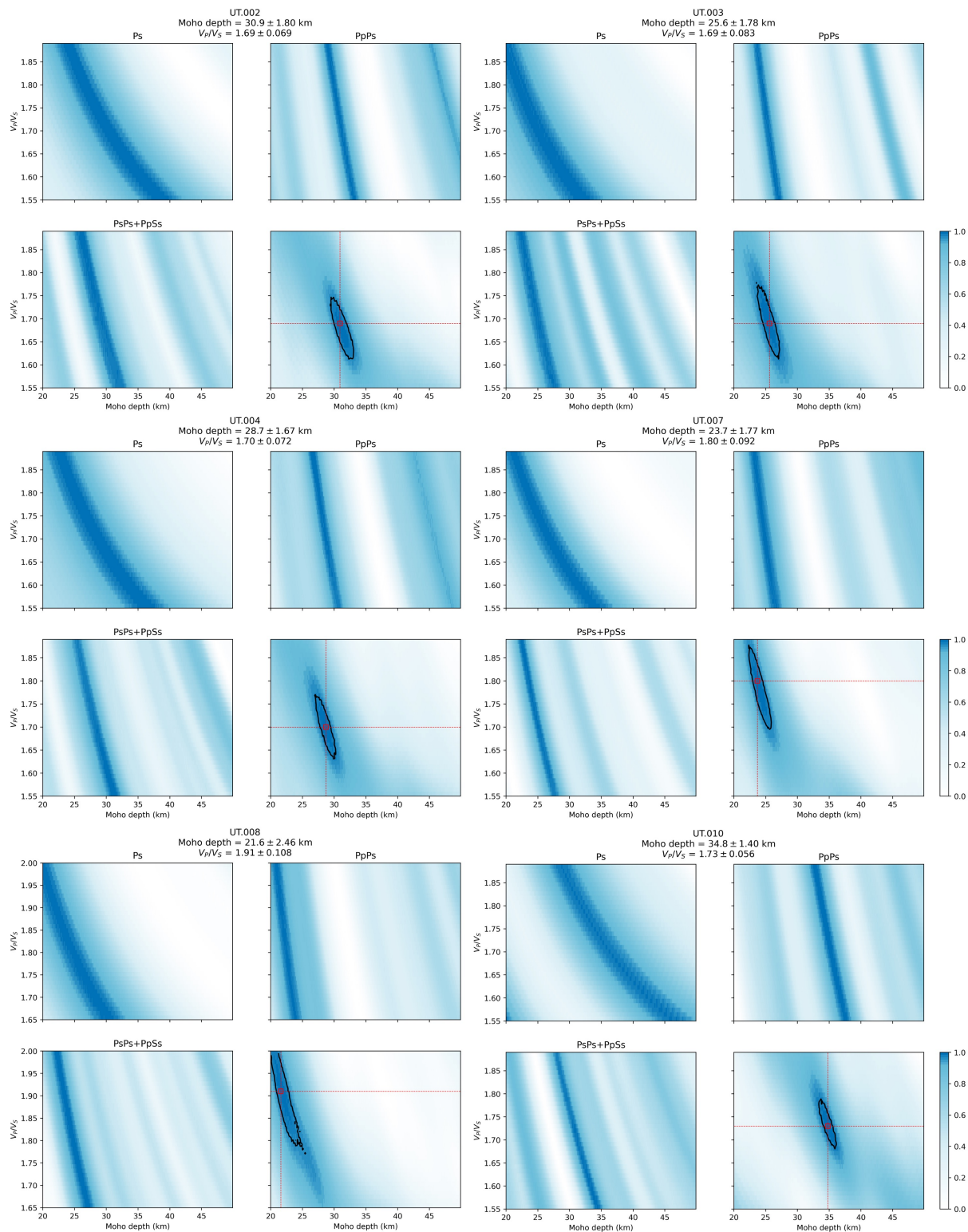
**Figure S19.** Results of the H-k stacking process for 6 high-quality Lisard stations. Stack values in each panel are normalized from 0 to 1.
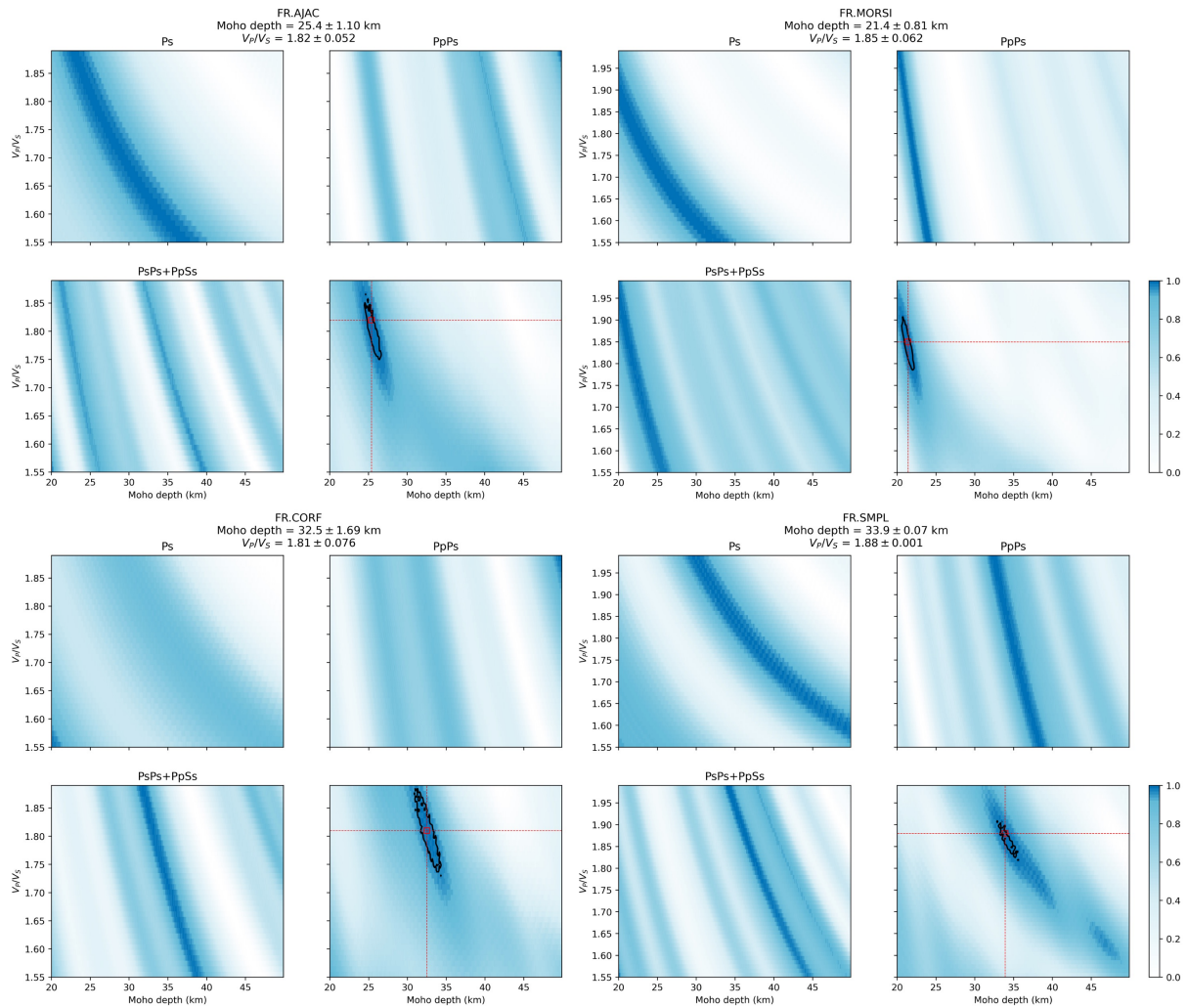
Figure S20. Results of the H-k stacking process for 4 public stations in Corsica of the French (RESIF) network.

Figure S21. Results of the H-k stacking process for 5 public stations in Sardinia and 1 in Elba Island of the Italian (INGV) and the Mediter-ranean (MedNet) networks.

22
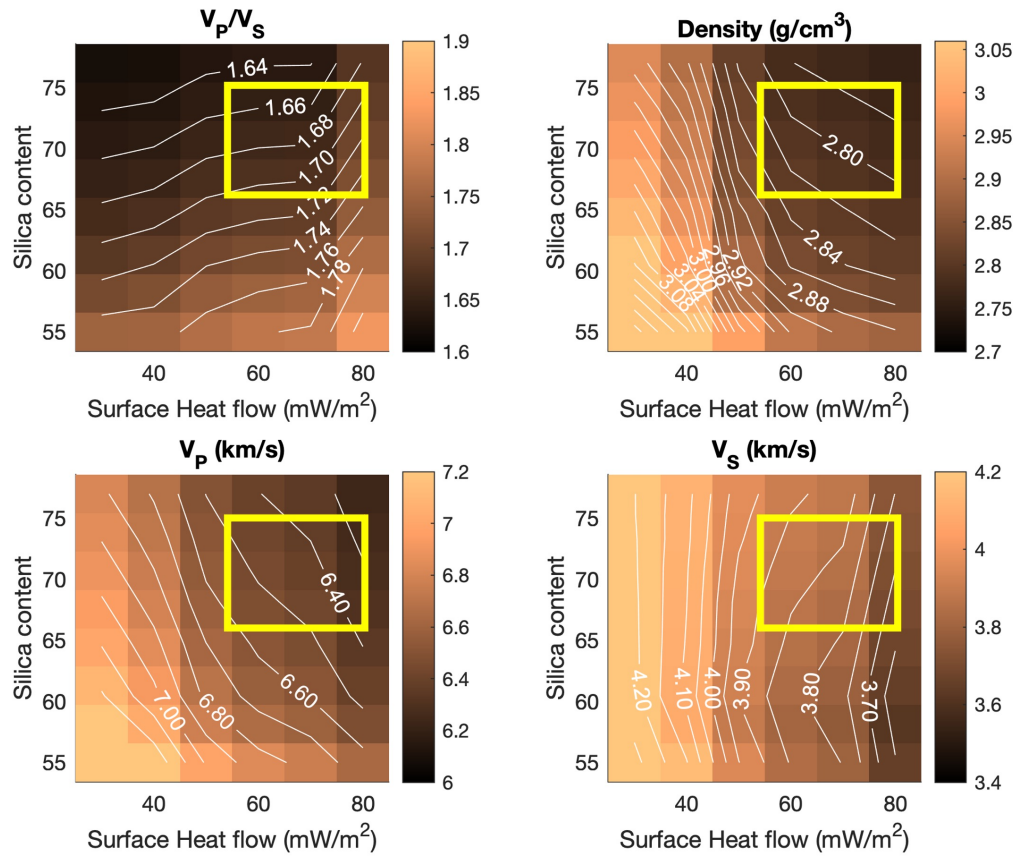
Figure S22. Effect of temperature and silica content on average V_P/V_S, absolute velocities and density of the crust. The values refer to the chemical compositions in Table 2, and have been calculated for a reference crust with a total depth of 30 km, but we vary the chemical compositions only in the top upper part (15 km). The rest is fixed and we use the reference middle- and lower-crust of Rudnick and Gao from 15 to 22 and from 22 to 30km, respectively. Thermal structures are, as in Fig. 11 of main paper, based on continental geotherms at variable heat-flow. In yellow, we indicate the range which satisfy the physical properties as constrained by geophysical studies.